Dynamic sample imaging in coherent diffractive imaging

Jesse N. Clark,[1,3,5,*] Corey T. Putkunz,[1,3] Evan K. Curwood,[2,3] David J. Vine,[2,3] Robert Scholten,[2,3] Ian McNulty,[4] Keith A. Nugent,[2,3] and Andrew G. Peele[1,3]

[1]*Department of Physics, La Trobe University, Victoria 3086, Australia*

[2]*School of Physics, University of Melbourne, Victoria 3010, Australia*

[3]*Australian Research Council Centre of Excellence for Coherent X-ray Science, Melbourne, Australia*

[4]*Advanced Photon Source, Argonne National Laboratory, Argonne, Illinois 60439, USA*

[5]*Currently with London Centre for Nanotechnology, University College, London WC1E 6BT, UK*

**Corresponding author: jesse.clark@ucl.ac.uk*

Received February 24, 2011; accepted March 30, 2011;
posted April 15, 2011 (Doc. ID 143250); published May 20, 2011

As the resolution in coherent diffractive imaging improves, interexposure and intraexposure sample dynamics, such as motion, degrade the quality of the reconstructed image. Selecting data sets that include only exposures where tolerably little motion has occurred is an inefficient use of time and flux, especially when detector readout time is significant. We provide an experimental demonstration of an approach in which all images of a data set exhibiting sample motion are combined to improve the quality of a reconstruction. This approach is applicable to more general sample dynamics (including sample damage) that occur during measurement. © 2011 Optical Society of America

OCIS codes: 100.5070, 100.3010, 110.7440, 180.7460.

Lensless imaging [1–3] approaches, sometimes known as coherent diffractive imaging (CDI), obtain the phase of the exit surface wave from a sample, potentially at wavelength-limited resolution. Coherent diffractive imaging has been demonstrated for materials [4] and biological [5] samples in two and three dimensions [6] using third generation synchrotron [7], high harmonic generation [8], and free electron laser sources [9].

As noncrystalline samples scatter a relatively small number of photons to large angles, high incident flux is necessary to achieve high spatial resolution. Assuming a partially coherent source, the flux incident on the sample can be increased by accepting more spatial modes from the source (lower spatial coherence) or by accepting more temporal modes (greater bandwidth). It has been shown that by treating the illumination as an incoherent sum of temporal [10,11] and/or spatial [12] modes, it is possible to suitably modify the reconstruction algorithm. A third approach to increase flux at the sample is to increase the exposure time. However, this can lead to increased sample drift during the measurement, resulting in a blurred diffraction pattern. This is an acute problem for techniques such as Fresnel CDI (FCDI) [7] and ptychography [13,14] that use knowledge of the position and form of the probe beam as part of the reconstruction algorithm. A common suggestion to deal with this problem is to phase subsets of the collected data, shift the resulting exit surface wave, and sum the results. However, this approach results in reconstructions that contain stochastic information beyond a given spatial frequency. Summing these does not improve the resolution of the final image. The present Letter theoretically and experimentally demonstrates that the diffraction pattern can be constructed from the known incident wave and the sample trajectory. We note that a theoretical approach based on using the autocorrelation of the data to separate the illumination and the sample function under conditions where the object is smaller than the support provided by the beam has been suggested and tested in simulation [15]. We show here that our approach can be applied without specific knowledge of the actual motion or requiring the sample to be smaller than the support. Finally, we note that the same principles can be applied to certain cases of sample damage during exposure [16].

Consider a sample illuminated by an x-ray beam: the wave in a plane immediately after the sample is described under the projection or Born approximations by

$$\psi(\boldsymbol{r}) = \psi_i(\boldsymbol{r})T(\boldsymbol{r}) = \psi_i(\boldsymbol{r}) + \psi_s(\boldsymbol{r}), \tag{1}$$

where $\boldsymbol{r}$ is the two-dimensional sample plane coordinate, the quantities subscripted i and s represent incident and scattered waves, respectively, and T is the complex sample transmission function. In the Fresnel approximation [17], omitting constant prefactors, the scattered wave in a detector plane when the sample has moved relative to the illumination by an amount $\boldsymbol{r}_0$ is

$$\hat{\psi}_s(\boldsymbol{\rho}, \boldsymbol{r}_0) = \int [T(\boldsymbol{r} - \boldsymbol{r}_0) - 1]\psi_i(\boldsymbol{r}) \exp\left[\frac{i\pi \boldsymbol{r}^2}{\lambda z_{\mathrm{sd}}}\right] \times \exp\left[\frac{-i2\pi \boldsymbol{r}\cdot\boldsymbol{\rho}}{\lambda z_{\mathrm{sd}}}\right] \mathrm{d}\boldsymbol{r}, \tag{2}$$

where λ is the wavelength of the radiation, z_{sd} is the sample to detector distance, and $\boldsymbol{\rho}$ is the two-dimensional detector plane coordinate. The net intensity resulting from sample motion during data collection is an incoherent sum of the intensities at the relative position of each exposure:

$$\langle I(\boldsymbol{\rho})\rangle = \sum_{w=1}^{W} |\hat{\psi}(\boldsymbol{\rho}, \boldsymbol{r}_w)|^2, \tag{3}$$

where W is the total number of positions and $\boldsymbol{r}_w$ is the shift of the sample relative to the illumination for each position. Treating the intensity as the incoherent sum of sample positions allows the motion to be incorporated

 © 2011 Optical Society of America

into the phase retrieval algorithm in an almost identical fashion to methods for incorporating the effects of partial coherence [10–12]. Consider the case of spherical illumination, $\psi_i(\boldsymbol{r}) = \exp[i\pi \boldsymbol{r}^2/\lambda z_{\mathrm{fs}}]$, where z_{fs} is the source to sample distance. It can be shown that

$$\hat{\psi}_s(\boldsymbol{\rho}, \boldsymbol{r}_0) = \exp[C(\boldsymbol{r}_0^2 - 2\boldsymbol{r}_0 \cdot \boldsymbol{\rho})]\hat{\psi}_s(\boldsymbol{\rho} - M\boldsymbol{r}_0), \quad (4)$$

where $C = (i\pi M)/(\lambda z_{\mathrm{sd}})$ and $M = (z_{\mathrm{sd}} + z_{\mathrm{fs}})/z_{\mathrm{fs}}$. Consequently, the diffracted intensity for a given sample position is

$$I(\boldsymbol{\rho}, \boldsymbol{\rho}_0) = |\hat{\psi}_i(\boldsymbol{\rho})|^2 + |\hat{\psi}_s(\boldsymbol{\rho} - \boldsymbol{\rho}_0)|^2 + 2|\hat{\psi}_i(\boldsymbol{\rho})||\hat{\psi}_s(\boldsymbol{\rho} - \boldsymbol{\rho}_0)|\cos(\theta(\boldsymbol{\rho} - \boldsymbol{\rho}_0)), \quad (5)$$

where $\boldsymbol{\rho}_0 = M\boldsymbol{r}_0$, and $\theta(\boldsymbol{\rho})$ represents the departure in the transmitted wave from the phase curvature of the incident wave. In the limit of many positions, which are assumed close enough that the amplitude of the illumination can be considered constant, the diffracted intensity can be written using convolutions with $\eta(\boldsymbol{\rho})$, the sample trajectory measured in the detector plane:

$$\langle I(\boldsymbol{\rho})\rangle = W|\hat{\psi}_i(\boldsymbol{\rho})|^2 + W\eta(\boldsymbol{\rho}) \otimes |\hat{\psi}_s(\boldsymbol{\rho})|^2 + 2W|\hat{\psi}_i(\boldsymbol{\rho})|\eta(\boldsymbol{\rho}) \otimes |\hat{\psi}_s(\boldsymbol{\rho})|\cos(\theta(\boldsymbol{\rho})). \quad (6)$$

If we also assume that about each exposure position, $\boldsymbol{r}_w$, there is small-scale random motion that takes place during the exposure, we can combine the modal approach of Eq. (3) and the convolution approach of Eq. (6) to then write the recorded intensity as

$$\langle I(\boldsymbol{\rho})\rangle = W|\hat{\psi}_i(\boldsymbol{\rho})|^2 + A(\boldsymbol{\rho}) + 2|\hat{\psi}_i(\boldsymbol{\rho})|B(\boldsymbol{\rho}), \quad (7)$$

where $A(\boldsymbol{\rho}) = [\sum_{w=1}^{W} |\hat{\psi}_s(\boldsymbol{\rho}, \boldsymbol{\rho}_w)|^2] \bigotimes \eta(\boldsymbol{\rho})$, $B(\boldsymbol{\rho}) = [\sum_{w=1}^{W} |\hat{\psi}_s(\boldsymbol{\rho}, \boldsymbol{\rho}_w)|\cos(\theta(\boldsymbol{\rho}, \boldsymbol{\rho}_w))] \bigotimes \eta(\boldsymbol{\rho})$, and W represents the discrete exposure positions. Here the summation terms account for the large-scale motion by approximating it with a series of discrete positions corresponding to each exposure, and the convolution accounts for the small-scale motion by approximating it as a continuous random motion within an exposure. In FCDI it is possible to obtain an estimate of the magnified sample position based on the holographic image of the sample in each exposure. From this a discrete set of sample positions can be obtained that can be used in Eq. (7) to form the diffracted intensity. In some cases the sample trajectory may not be known. Here we model the unknown trajectory (or uncertainty) as $\eta(\boldsymbol{\rho}, \boldsymbol{\sigma})$, where $\boldsymbol{\sigma}$ represents the free parameters in the model. We can then, as a function of $\boldsymbol{\sigma}$, minimize the quantity $E_k = \int |\langle I(\boldsymbol{\rho})\rangle - \langle I^k(\boldsymbol{\rho}, \boldsymbol{\sigma}^k)\rangle| \mathrm{d}\boldsymbol{\rho}$ to obtain the kth estimate for the free parameters, $\boldsymbol{\sigma}^k$, from which the corresponding estimate for the intensity can be constructed using Eq. (7) and $\eta(\boldsymbol{\rho}, \boldsymbol{\sigma}^k)$. The modulus constraint is now applied as

$$\hat{\psi}^{k'}(\boldsymbol{\rho}, \boldsymbol{\rho}_p) = \left(\frac{\langle I(\boldsymbol{\rho})\rangle}{\langle I^k(\boldsymbol{\rho})\rangle}\right)^{\frac{1}{2}} \hat{\psi}^k(\boldsymbol{\rho}, \boldsymbol{\rho}_p), \quad (8)$$

where $\boldsymbol{\rho}_p$ is the single sample position to propagate back, a logical choice being the position in which the sample spends the most time.

To demonstrate dynamic sample imaging in CDI, we carried out an experiment at beamline 2-ID-B [18] at the Advanced Photon Source. Monochromatic 2.5 keV x rays illuminated a 160 μm diameter Fresnel zone plate with a 50 nm outer zone width and a focal length of 16.3 mm. A central stop in conjunction with an order sorting aperture removed unwanted diffraction orders, allowing only the first-order focused beam to illuminate the sample, placed 1 mm from the focus. A Princeton Instruments peltier cooled CCD with 2048×2048 13.5 μm square pixels detected the diffraction patterns 0.8 m downstream from the sample. The x-ray beam remained *in vacuo*, aside from a 1 cm air gap between the beamline exit window and the entrance window for the end station approximately 2.4 m upstream of the zone plate. The beamline monochromator exit slit was adjusted so as to coherently illuminate the zone plate [19]. The sample consisted of a gold resolution pattern with a thickness of 150 ± 15 nm supported on a 100 nm Si_3N_4 membrane. A data set consisting of 700×1 s exposures was collected, and the resultant diffraction pattern is shown in Fig. 1(a). A coarse sample trajectory was determined by dividing the data into subsets of five exposures and iteratively

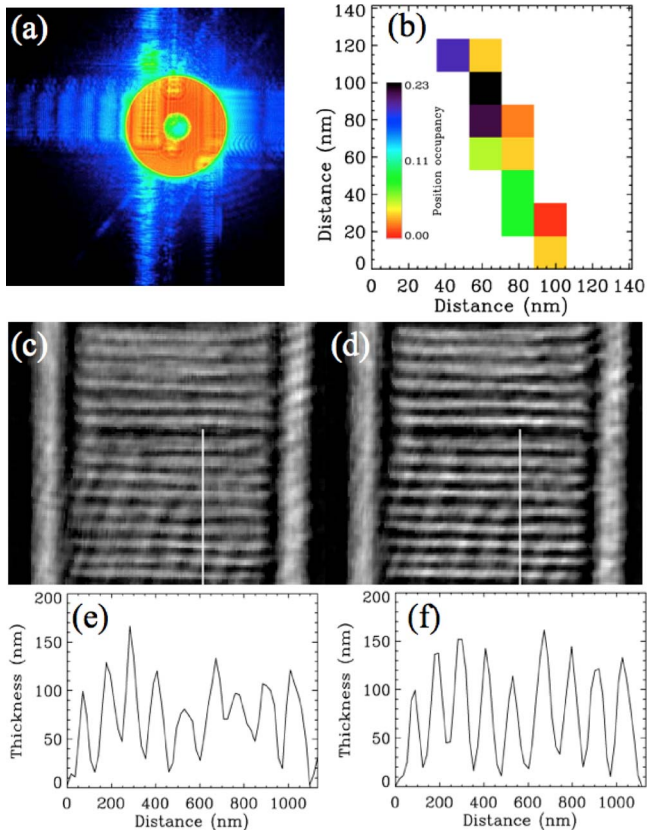

Fig. 1. (Color online) (a) Diffraction pattern for sample with motion, (b) calculated sample trajectory (the color bar indicates the relative number of exposures for a given sample position), (c) reconstructed thickness with no motion correction, (d) reconstruction using the calculated positions and refined using an unknown sample uncertainty with a normal distribution, (e) and (f) lineouts corresponding to (c) and (d), respectively.

reconstructing the hologram [7]. From these reconstructions the relative translations of the sample can be easily determined. The resulting trajectory is shown in Fig. 1(b) and shows the sample drifted by about 125 nm during the data collection. Figure 1(c) shows a reconstructed region of the sample using no motion correction, while Fig. 1(d) shows the result for motion correction using the coarse sample positions coupled with the minimization step based on a model of normally distributed uncertainty for the sample positions. The reconstructions were run for 200 iterations using error reduction [2] with a shrink-wrap support [20] and a complex constraint [21]. Line-outs as indicated by the bars in the images are also shown at Figs. 1(e) and 1(f). There is significant improvement in the nominally binary pattern using the measured positions coupled with the minimization refinement procedure. The recovered thickness agrees well with the specified value of 150 ± 15 nm.

Our results show significant improvement in the recovered thickness where the sample motion during the exposure series was much greater than the lateral spatial resolution of the reconstruction. This is on the order of magnitude of sample drifts commonly seen due to thermal effects in high resolution x-ray imaging experiments. In addition, sensitivity to drift may be aggravated using slow detectors such as CCDs. The approach described here is a powerful way to maximize the use of data collected under these conditions.

We acknowledge the support of the Australian Research Council Centre of Excellence for Coherent X-ray Science and the Australian Synchrotron Research Program. Use of the Advanced Photon Source is supported by the U.S. Department of Energy (DOE) Office of Science and Office of Basic Energy Sciences under Contract No. DE-AC02-06CH11357.

References

1. R. Gerchberg and W. Saxton, Optik **35**, 237 (1972).
2. J. R. Fienup, Appl. Opt. **21**, 2758 (1982).
3. J. Miao, P. Charalambous, J. Kirz, and D. Sayre, Nature **400**, 342 (1999).
4. G. J. Williams, M. A. Pfeifer, I. A. Vartanyants, and I. K. Robinson, Phys. Rev. Lett. **90**, 175501 (2003).
5. D. Shapiro, P. Thibault, T. Beetz, V. Elser, M. Howells, C. Jacobsen, J. Kirz, E. Lima, H. Miao, A. M. Neiman, and D. Sayre, Proc. Natl. Acad. Sci. USA **102**, 15343 (2005).
6. H. N. Chapman, A. Barty, S. Marchesini, A. Noy, S. P. Hau-Riege, C. Cui, M. R. Howells, R. Rosen, H. He, J. C. H. Spence, U. Weierstall, T. Beetz, C. Jacobsen, and D. Shapiro, J. Opt. Soc. Am. A **23**, 1179 (2006).
7. G. J. Williams, H. M. Quiney, B. B. Dhal, C. Q. Tran, K. A. Nugent, A. G. Peele, D. Paterson, and M. D. de Jonge, Phys. Rev. Lett. **97**, 025506 (2006).
8. R. L. Sandberg, A. Paul, D. A. Raymondson, S. Hadrich, D. M. Gaudiosi, J. Holtsnider, R. I. Tobey, O. Cohen, M. M. Murnane, and H. C. Kapteyn, Phys. Rev. Lett. **99**, 098103 (2007).
9. H. N. Chapman, A. Barty, M. J. Bogan, S. Boutet, M. Frank, S. P. Hau-Riege, S. Marchesini, B. W. Woods, S. Bajt, W. H. Benner, R. A. London, E. Plonjes, M. Kuhlmann, R. Treusch, S. Dusterer, T. Tschentscher, J. R. Schneider, E. Spiller, T. Moller, C. Bostedt, M. Hoener, D. A. Shapiro, K. O. Hodgson, D. van der Spoel, F. Burmeister, M. Bergh, C. Caleman, G. Huldt, M. M. Seibert, F. R. N. C. Maia, R. W. Lee, A. Szoke, N. Timneanu, and J. Hajdu, Nat. Phys. **2**, 839 (2006).
10. B. Chen, R. A. Dilanian, S. Teichmann, B. Abbey, A. G. Peele, G. J. Williams, P. Hannaford, L. Van Dao, H. M. Quiney, and K. A. Nugent, Phys. Rev. A **79**, 023809 (2009).
11. R. A. Dilanian, B. Chen, G. J. Williams, H. M. Quiney, K. A. Nugent, S. Teichmann, P. Hannaford, L. V. Dao, and A. G. Peele, J. Appl. Phys. **106**, 023110 (2009).
12. L. W. Whitehead, G. J. Williams, H. M. Quiney, D. J. Vine, R. A. Dilanian, S. Flewett, K. A. Nugent, A. G. Peele, E. Balaur, and I. McNulty, Phys. Rev. Lett. **103**, 243902 (2009).
13. J. M. Rodenburg and R. H. T. Bates, Phil. Trans. R. Soc. Lond. A **339**, 521 (1992).
14. C. T. Putkunz, J. N. Clark, D. J. Vine, G. J. Williams, M. A. Pfeifer, E. Balaur, I. McNulty, K. A. Nugent, and A. G. Peele, Phys. Rev. Lett. **106**, 013903 (2011).
15. A. V. Martin, L. J. Allen, and K. Ishizuka, Ultramicroscopy **110**, 359 (2010).
16. H. M. Quiney and K. A. Nugent, Nat. Phys. **7**, 142 (2011).
17. J. W. Goodman, *Introduction to Fourier Optics*, 2nd ed. (McGraw-Hill, 1996).
18. I. McNulty, A. Khounsary, Y. P. Feng, Y. Qian, J. Barraza, C. Benson, and D. Shu, Rev. Sci. Instrum. **67**, 3372 (1996).
19. C. Q. Tran, A. G. Peele, A. Roberts, K. A. Nugent, D. Paterson, and I. McNulty, Opt. Lett. **30**, 204 (2005).
20. S. Marchesini, H. He, H. N. Chapman, S. P. Hau-Riege, A. Noy, M. R. Howells, U. Weierstall, and J. C. H. Spence, Phys. Rev. B **68**, 140101 (2003).
21. J. N. Clark, C. T. Putkunz, M. A. Pfeifer, A. G. Peele, G. J. Williams, B. Chen, K. A. Nugent, C. Hall, W. Fullagar, S. Kim, and I. McNulty, Opt. Express **18**, 1981 (2010).